Monatshefte für Chemie 135, 1189–1199 (2004)
DOI 10.1007/s00706-004-0191-9

Monatshefte für Chemie
Chemical Monthly
Printed in Austria

Synthesis, Conformation, and Metabolism of a Selenium Bilirubin

Brahmananda Ghosh[1], **David A. Lightner**[1,*], and **Antony F. McDonagh**[2,*]

[1] Department of Chemistry, University of Nevada, Reno, Nevada 89557-0020, USA
[2] G.I. Unit and Liver Center, University of California, San Francisco, California 94143-0538, USA

Received February 12, 2004; accepted February 17, 2004
Published online July 23, 2004

Summary. A symmetrical C(10)-selena-bilirubin analog, 8,12-bis(2-carboxyethyl)-7,13-dimethyl-2,3,17,18-tetraethyl-10-selenabiladiene-*ac*-1,19(21*H*,24*H*)-dione was synthesized from 8-(2-carboxyethyl)-2,3-diethyl-7-methyl-(10*H*)-dipyrrin-1-one in one step by reaction with diselenyl dichloride. The selena-rubin exhibited *UV-vis* and *NMR* spectroscopic properties similar to those of the parent mesobilirubin, and like bilirubin and mesobilirubin, it adopts an intramolecularly hydrogen-bonded conformation, shaped like a ridge-tile but with a steeper pitch. The longer C–Se bond lengths (2.2 Å) and smaller bond angles at C–Se–C (88°), as compared to C–CH_2–C (∼1.5 Å, ∼106°), lead to an interplanar angle between the two dipyrrinones of only 72°, which is considerably less than that of bilirubin (∼100°) and close to that (74°) of its 10-thia-rubin analog. Despite the conformational distortion, the sensitivity of Se toward oxidation and the typically weak C–Se bond, the selena-rubin is metabolized in normal rats, like bilirubin, to acyl glucuronides, which are secreted into bile. In mutant (*Gunn*) rats lacking bilirubin glucuronosyl transferase (*UGT1A1*), glucuronide or other metabolites of the selena-rubin were not detected in bile, demonstrating the importance of hepatic glucuronidation for its biliary excretion.

Keywords. Pyrrole; Hydrogen bonding; Conformational analysis; Metabolism.

Introduction

Bilirubin is a "linear" tetrapyrrole [1, 2] and the hydrophobic, yellow-orange cytotoxic pigment of jaundice [2, 3]. Like a two-bladed molecular propeller, it is composed of two dipyrrinones, conjoined to a CH_2 group (Fig. 1A). Bilirubin and its analogs with vinyl groups replaced by ethyls have unusual lipid solubility and solution properties which stem from tenacious hydrogen bonding between the dipyrrinones and the propionic acids. Each dipyrrinone can rotate independently

* Corresponding authors. E-mails: lightner@scs.unr.edu, tonymcd@itsa.ucsf.edu

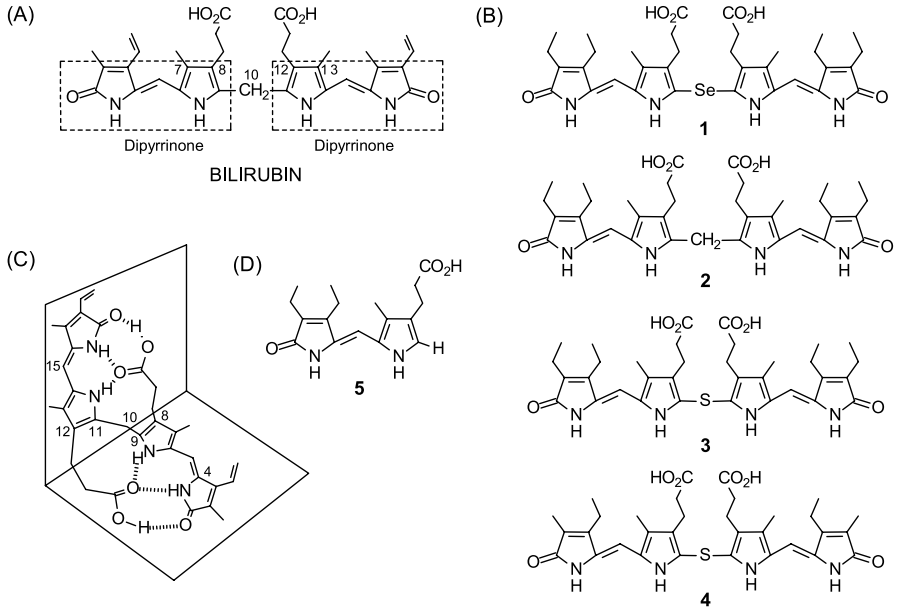

Fig. 1. (A) Linear representation of bilirubin showing its two dipyrrinone chromophores conjoined to the C(10)–CH_2; (B) the target selena-rubin **1** and its structurally related 2,18-homomesobilirubin (**2**) and thia-rubin **3** analogues and thia-mesobilirubin-XIIIα (**4**); (C) the most stable conformation of bilirubin, shaped like a ridge-tile with intramolecular hydrogen bonds (dashed lines) between the dipyrrinones and propionic acid groups; (D) the dipyrrinone precursor **5** to rubins **1**–**3**

about the central C(10)–CH_2 group, thereby bringing it within intramolecular hydrogen bonding distance of a propionic acid. This leaves the polar acid and lactam groups tucked inside a conformation shaped like a half-opened book (or ridge-tile) and dotted with hydrophobic hydrocarbon groups on the periphery (Fig. 1C) [4]. The ridge-tile conformation, secured by six intramolecular hydrogen bonds, dominates the stereochemistry of bilirubin and its vinyl-reduced analog, mesobilirubin [5], and explains their lipophilicity and poor secretion across the liver into bile [3, 6]. Bilirubin can become toxic if it accumulates in the body. Normally, this does not happen to any marked degree because the pigment is converted enzymically in the liver to mono- and diglucuronide metabolites that are less lipophilic and are efficiently eliminated in bile [1, 3]. Translocation of bilirubin glucuronides from the liver into bile across the canalicular membrane of the hepatocyte is believed to be effected by the *ATP*-dependent glycoprotein *MRP2* (multi-drug resistance protein 2) [7]. Bilirubin itself is hydrophobic and is not excreted significantly in bile or urine [3c].

In earlier investigations of the importance of the 3-dimensional molecular structure of bilirubin to its metabolism, we constructed bilirubin analogues designed to alter the pigment's lipophilicity by substitution at C(10) [8–10], the ''hinge'' of the ridge-tile conformation (Fig. 1C). For example, with an oxo group at C(10), the bilirubin becomes more polar and much less soluble in chloroform than bilirubin [10] – and is excreted by the liver into bile both as a glucuronide and as the intact pigment. In contrast, with a *gem*-dimethyl at C(10), the rubin becomes amphiphilic and easily soluble in both chloroform and methanol [8a], yet is metabolized in the usual way [9]. Replacing the C(10)–CH_2 group with an S atom causes

the pigment (**3**, Fig. 1B) to distort into a steeper pitch ridge-tile because of the smaller C–S–C bond angle and larger C–S bond distance. Despite this, the only known thia-rubin **3** that has been studied has been shown to be metabolized and excreted just like that of bilirubin [11].

To further alter the interplanar angle of the ridge-tile structure, we synthesized the first selena-rubin **1**, with a selenium atom replacing the C(10)–CH_2 group of a mesobilirubin **2**. Like bilirubin, **1** (Fig. 1B) is predicted by molecular modeling (Sybyl) to engage in intramolecular hydrogen bonding – despite the long C–Se bonds connecting the two dipyrrinones to the C(10) selenium atom and the small C–Se–C bond angle. To our knowledge, **1** is the first example of a selena-bilirubin. In the following, we describe its synthesis and metabolic disposition in normal rats and in homozygous *Gunn* rats lacking bilirubin conjugating activity.

Results and Discussion

Synthesis Aspects

Our recent studies showing that 10-thia-mesobilirubins could be prepared by reaction of 9-H dipyrrinones with SCl_2 [11] suggested that dithia (or diselena) analogs might be synthesized by reaction of a suitable dipyrrinone with S_2Cl_2 (or Se_2Cl_2). In order to test this hypothesis, we attempted to condense the readily available 9-H dipyrrinone **5** (Fig. 1D), previously prepared in our laboratory [9a, 11a] and possessing the requisite β-substituents, with S_2Cl_2. However, the reaction gave not the disulfide but thia-rubin **3** (Fig. 1B) as the only product. We were not surprised then that reaction with Se_2Cl_2 smoothly transformed **5** into a new tetrapyrrole, which we assumed to be **1** – (but could have been the diselenide analog).

Molecular Structure

The constitution of **1** follows from the previously established structure of its dipyrrinone precursor, **5**. There remained only a question as to whether a mono- or diselenide had been formed. Combustion analyses and FAB-HRMS confirmed that but one Se atom was present. Further confirmation of the structure of **1** comes from ^{13}C NMR spectroscopy (Table 1). Noteworthy is the absence of the ^{13}C NMR signal for the C(10)–CH_2 usually found in bilirubins near 23.5 ppm in *DMSO*-d_6 and near 22.5 ppm in $CDCl_3$ [5]. Otherwise, there are no striking differences in ^{13}C NMR chemical shifts between rubins with a C(10)–CH_2 and those with C(10) replaced by either Se(10) or S(10). Surprisingly, perhaps, ring carbons 9(11) of **1**–**3** have essentially the same chemical shift, whether with a selenium or sulfur substituent present. All carbons of the propionic acid chains have very similar chemical shifts, as expected, as do ring carbons 8(10), 7(13) and 3(17). However, ring carbons 2(18) and the bridging carbons 5(15) are more shielded in **1** and **3** than in **2**, but ring carbons 4(16) and 6(14) are more deshielded. And carbons 8(12) are more shielded in **1** than in **3**.

The ^1H NMR spectrum of **1** is also consistent with its constitutional structure. Most significantly, the C(10)–CH_2 signal seen in bilirubin and mesobilirubin **2** near 4 ppm is absent, and the C(9) hydrogen of the starting dipyrrinone **5** near 6.6–6.9 ppm is also absent.

Table 1. Comparison of ^{13}C NMR chemical shifts[a] (ppm) and assignments of selena-rubin **1**, mesobilirubin **2**, and thia-rubin **3**

Carbon	δ (ppm) in *DMSO*-d_6			δ (ppm) in $CDCl_3$		
	1	**2**	**3**[b]	**1**	**2**	**3**[b]
1, 19	171.80	171.50	171.80	174.7	174.7	174.8
2, 18	126.25	128.73	125.40	127.8	128.5	127.0
2^1, 18^1	16.35	16.20	16.35	16.68	16.69	16.68
2^2, 18^2	13.77	13.60	13.75	13.84	13.77	13.84
3, 17	146.83	146.65	146.80	147.8	147.9	147.8
3^1, 17^1	16.94	16.85	16.93	17.65	17.71	17.76
3^2, 17^2	15.65	15.46	15.65	15.76	15.70	15.76
4, 16	130.0	127.8	130.1	129.3	129.4	129.3
5, 15	96.83	97.80	96.72	99.55	100.57	99.53
6, 14	127.4	122.25	126.3	127.1	123.6	126.2
7, 13	121.7	122.04	121.8	123.1	124.6	123.7
7^1, 13^1	9.40	9.00	9.35	10.46	10.03	10.46
8, 12	115.31	119.22	119.5	119.6	119.5	123.4
8^1, 12^1	20.80	19.20	19.95	20.2	18.63	19.17
8^2, 12^2	34.50	34.35	34.23	32.31	32.72	32.15
8^3, 12^3	173.84	173.82	173.80	178.9	179.5	179.1
9, 11	130.2	130.1	130.4	129.9	133.2	130.0
10	–	25.0	–	–	29.7	–

[a] In ppm downfield from *TMS* for 1×10^{-3} *M* solutions; [b] entries for **3** obtained from Ref. [14]

Conformation

$^1H\{^1H\}$-Nuclear *Overhauser* effects (N*O*Es) are found between the lactam and pyrrole NHs of **1** in $CDCl_3$, and between the C(5)/C(15) vinyl hydrogens and the C(7)/C(13) methyls and the C(3)/C(17) ethyl group methylenes (Fig. 2). These data indicate a *syn-Z* configuration at the exocyclic double bonds at C(4) and C(15). In addition, a weaker N*O*E is seen between the lactam NHs and the propionic acid COOHs in **1**, indicating that they are in close proximity – as would be expected [4c, 12] from an intramolecularly hydrogen-bonded ridge-tile conformation (as in Fig. 1C). Further support for such a conformation for **1** in $CDCl_3$ comes from: (*i*) the observation of an ABCX coupling pattern in the propionic acid

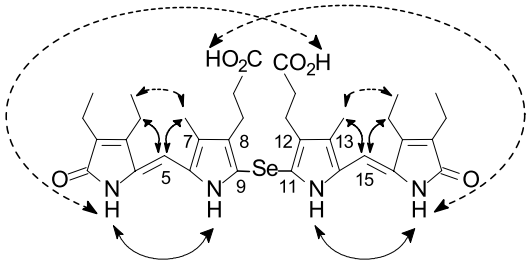

Fig. 2. N*O*Es found for selena-rubin **1** are shown by curved, double-headed arrows; weak N*O*Es are shown by curved, dashed arrows

Table 2. ^{1}H NMR NH and COOH chemical shifts in $CDCl_3$ and *DMSO*-d_6 of selena-rubin **1**, mesobilirubin **2**, and thia-rubin **3**

Compound	δ (ppm) in *DMSO*-d_6			δ (ppm) in $CDCl_3$		
	N(21), N(24)	N(22), N(23)	COOH	N(21), N(24)	N(22), N(23)	COOH
1	9.94	10.76	11.98	10.84	9.70	13.60
2	9.78	10.32	11.90	10.59	9.14	13.67
3	9.99	10.73	11.96	10.94	9.89	13.61

–CH_2–CH_2– segment, with coupling constants characteristic of a fixed staggered geometry [4c], and (*ii*) the NH chemical shifts (Table 2) [5]. In *DSMO*-d_6 solvent the sets of NH and OH chemical shifts of **1**–**3** are essentially identical, match up well with those from other bilirubins, and are consistent with solvent participation in hydrogen bonding [2, 4c, 5, 8]. In contrast, the NH and OH chemical shifts in $CDCl_3$ are consistent with intramolecular hydrogen bonding, as depicted in Fig. 1C, with the chemical shifts found in bilirubin and other rubins with C(8) and C(12) propionic acid groups [2, 4c, 5, 8].

In addition to the NMR spectroscopic evidence on the conformation of selena-rubin **1**, molecular dynamics calculations (Sybyl) [13] support an intramolecularly hydrogen bonded ridge-tile conformation. Two isoenergetic ridge-tile conformations are found, corresponding to mirror image enantiomers (Fig. 3). The shapes of the ridge-tiles are generally similar to those found by molecular dynamics computations and by X-ray crystallography on bilirubin and mesobilirubins [4, 5]. The longer C(9)/C(11)–Se bond lengths (∼2.2 Å) and smaller C(9)–Se–C(11) bond angle (∼88°) of **1**, as compared to the C(9)/C(11)–CH_2 bond length (∼1.5 Å) and C(9)–CH_2–C(11) bond angle (∼106°) of mesobilirubin **2**, or even the

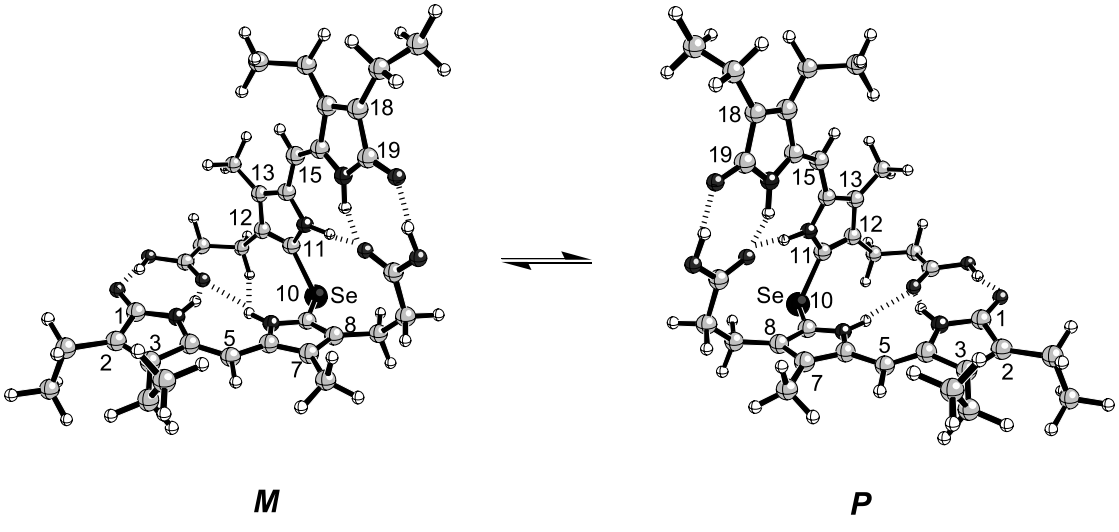

Fig. 3. Ball and Stick representations of the energy-minimized hydrogen-bonded structure of enantiomeric (*M*)- and (*P*)-helical conformations of 10-selena-rubin **1**; *d* [C(9)/C(11)–Se] = 2.2 Å; ∠C(9)–Se–C(11) = 88.2°; interplanar dihedral angle $\theta = 72°$

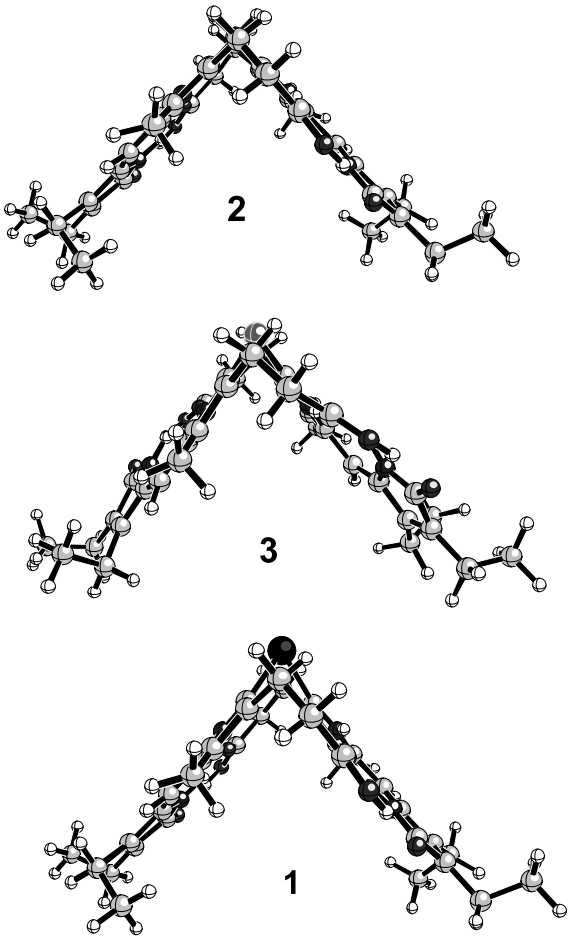

Fig. 4. Edge-view comparison of the ridge-tile conformations of 2,18-bis-homo-mesobilirubin-XIIIα (**2**, $\theta = 100°$), 10-thia-rubin **3** ($\theta = 74°$), and 10-selena-rubin **1** ($\theta = 72°$), where θ is the interplanar angle between the two dipyrrinones

C(9)–S–C(11) bond angle ($\sim$93°) and C(9)/C(11)–S bond lengths ($\sim$1.8 Å) of thia-rubin **3**, lead to a smaller interplanar (or dihedral) angle ($\theta \sim 72°$) between the two dipyrrinone planes as compared to mesobilirubin **2** or bilirubin ($\theta \sim 100°$). The dipyrrinones twist when necessary to engage in intramolecular hydrogen bonding to the propionic acids. Thus, the ridge-tile of **1** is more closed than that of **2** and adapted to a roof of steeper pitch than the corresponding mesobilirubin ridge-tile, as shown in Fig. 4 by the edge-view Ball and Stick [13] diagrams.

Polarity and Solubility

Figure 5 shows an *HPLC* chromatogram of a mixture of selena-rubin **1**, 2,18-homomesobilirubin (**2**), thia-rubin **3,** thia-mesobilirubin-XIIIα (**4**) [14], which is similar to thia-rubin **3** but has methyl groups at C(2) and C(18), and bilirubin. The corresponding relative retention times are 1.22, 1.18, 1.32, 1.11, and 1.00 min, indicating that **1** is slightly less polar than **2**, which is considerably more polar

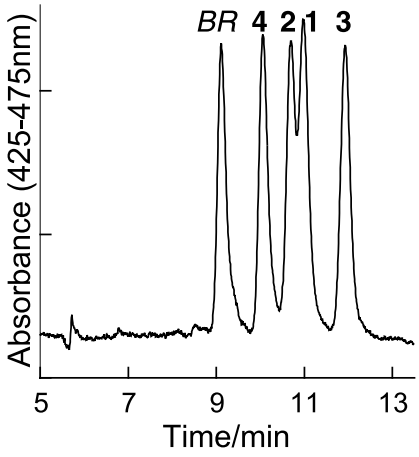

Fig. 5. Elution order of bilirubin (*BR*), 10-thia-mesobilirubin-XIIIα (**4**), 2,18-bis-homo-mesobilirubin-XIIIα (**2**), 10-selena-rubin **1**, and 10-thia-rubin **3** on reversed phase HPLC (constructed by combining normalized chromatograms of the individual pigments)

than **3**. It can be seen that replacing the C(10)–CH_2 by Se has only a small effect on R_t, whereas replacing the CH_2 or Se by S gives a markedly less polar pigment. The difference in R_t between thia-rubins **3** and **4** is consistent with the presence of two ethyl groups in **3** at C(2) and C(18) compared to two methyls at the corresponding positions in **4**. On silica TLC (solvent CH_2Cl_2:*Me*OH = 99:1), **1** and **3** have R_f values ~0.8, whereas that of **2** is ~0.75, suggesting very similar polarity. In contrast, the R_f of **4** is ~0.5, indicating greater polarity. Selena-rubin **1**, like bilirubin, mesobilirubin **2**, and thia-rubins **3** and **4**, is soluble in $CHCl_3$ and insoluble in dilute aq. $NaHCO_3$ solution. However, solubility in $CHCl_3$ is poorer for **1** than **2**, which might be attributed to the presence of the larger ''exposed'' Se atom to the solvent. Taken collectively, these characteristics are consistent with the propionic acid side chains being involved in intramolecular hydrogen bonding and unavailable for solvent interaction.

Hepatic Metabolism

Bilirubin is cleared efficiently from the circulation in healthy humans, rats, and many other mammals by the liver, where it undergoes enzymic conversion to two isomeric monoglucuronides [1, 3]. These are partly converted by the same enzyme to bilirubin diglucuronide. The resulting mixture of three acyl glucuronides is secreted from the liver into bile. Formation of the glucuronides is catalyzed by the glucuronosyl transferase enzyme *UGT1A1* (*UGT1.1*) [15–20]. When this enzyme is absent, as in the homozygous *Gunn* rat [15–17, 20], bilirubin glucuronides are not formed and only very low concentrations of the parent pigment and none of its glucuronides are excreted in bile. This causes accumulation of bilirubin in the circulation and extravascular tissues. The mechanism of bilirubin uptake into the liver from the circulation is controversial [21]. Efficient secretion of bilirubin glucuronides into bile depends on the presence of the *ABC*-transport protein *MRP2* (*ABCC2*) which is localized in the canalicular membrane of hepatocytes [22].

Although *MRP2* is thought to be a general organic anion canalicular transporter, it does not facilitate the biliary excretion of bilirubin, which is an organic anion at physiologic *pH*. The reason may be related to the conformation, intramolecular hydrogen bonding, and resulting lipophilic properties of bilirubin. Few rubins more lipophilic than bilirubin have previously been studied *in vivo*.

Compound **2** is a symmetrical, more heavily alkylated, analog of bilirubin. It is identical to selena-rubin **1** and to thia-rubin **3**, except for the CH_2 replacing the Se and S atoms. All three compounds are chromatographically less polar (more hydrophobic) than bilirubin (Fig. 5). As reported earlier [9, 11a], rubin **2** and the less polar thia-rubin **3** are metabolized in the rat just like bilirubin. Thus, they are not excreted significantly in bile following intravenous injection into homozygous *Gunn* rats, but are excreted rapidly as two glucuronides, presumably the mono- and di-, on similar treatment of normal rats. The considerably less polar thia-rubin **4** also was metabolized in the same way (data not shown). Despite its substantially smaller pitch, selena-rubin **1** behaved almost identically to bilirubin, to **2**, and to thia-rubins **3** and **4** *in vivo* in the rat (Fig. 6). After being injected intravenously, no significant excretion of the pigment in bile was evident in *Gunn* rats, but prompt excretion of two metabolites was seen in normal rats. Both metabolites were more polar than the parent pigment and were hydrolyzed by 1.0 *M* NaOH and by β-glucuronidase to the parent compound **1** (Fig. 7). Their absorption spectra resembled that of the parent pigment (Fig. 7) but showed the emergence of a shorter wavelength absorption band in progressing from the monoglucuronide to the diglucuronide that is characteristic of the glucuronides of bilirubin and mesobilirubin. On this evidence, coupled with the fact that they were not formed in *Gunn* rats, we conclude that the metabolites are the mono- and diglucuronide of selena-rubin. The most polar of the two metabolites, presumably the diglucuronide, eluted just ahead

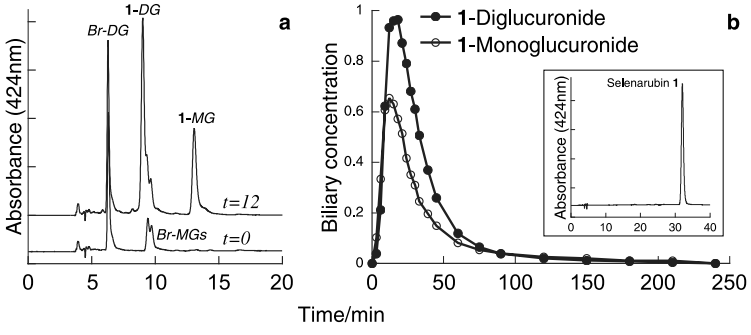

Fig. 6. Metabolism and biliary excretion of 10-selena-rubin **1** in the rat; panel **a**: HPLC chromatograms of bile collected before ($t = 0$) and 12 min after intravenous injection of **1** (0.25 mg in 1 cm^3 rat serum); at $t = 0$ the chromatogram shows the presence of bilirubin diglucuronide (main peak) and the two isomeric bilirubin monoglucuronides, which are not fully resolved under the chromatographic conditions used; no peaks were detectable at longer retention times (up to 40 min); panel **b**: biliary excretion profiles for the mono- and diglucuronides of **1**, derived from HPLC analyses of bile by plotting relative peak areas normalized to the maximum diglucuronide concentration; mean data from two experiments is shown; the inset in panel **b** shows a chromatogram, run under the same HPLC conditions as in panel **a**, of an aliquot of the serum solution of **1** injected into the animals

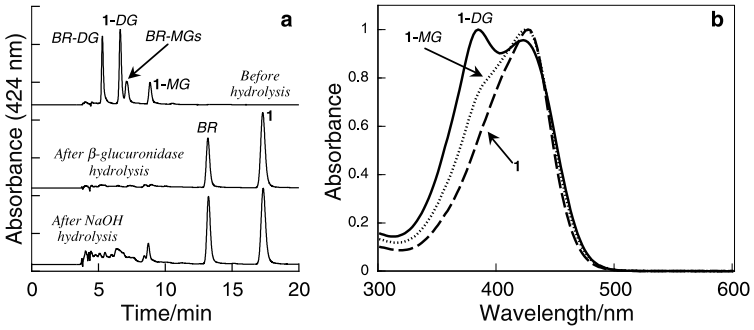

Fig. 7. Panel **a**: hydrolysis of glucuronides of **1** with β-glucuronidase and NaOH; samples of bile collected between 18 and 24 min after intravenous injection of a rat with **1** were analyzed by HPLC before and after treatment with β-glucuronidase or NaOH; *BR*, *BR-DG* and *BR-MGs* indicate endogenous bilirubin, bilirubin diglucuronide, and bilirubin monoglucuronides, respectively; chromatograms are normalized to maximum peak height; panel **b**: absorption spectra of **1** and its mono- (**1**-*MG*) and diglucuronide (**1**-*DG*); the spectra are normalized to maximum absorbance above 300 nm

of bilirubin monoglucuronides on *HPLC*, whereas the least polar eluted between the bilirubin monoglucuronides and unconjugated bilirubin.

Our results show that replacing the central methylene group of a close analog of bilirubin by selenium, thereby tightening the pitch of the favored ridge-tile conformation does not markedly hinder its glucuronidation *in vivo* by *UGT1A1*. Selena-rubin **1**, like bilirubin, rubin **2** and the thia rubins **3** and **4**, is taken up rapidly from the circulation into the liver, but is not transported into bile by *MRP2* or other canalicular membrane transporters. In contrast, its glucuronides, like those of bilirubin and **2** and **3**, are secreted promptly in bile. Presumably, the mechanisms involved in the hepatic uptake of **1** and **2** and in the biliary excretion of their glucuronides are the same as those involved in the uptake of bilirubin and excretion of its glucuronides. In the homozygous *Gunn* rat, where glucuronides were not formed, there was no detectable excretion of other colored metabolites of **1** and **3** in bile over the time period studied (4 h). Thus, these compounds are probably not good substrates for *UGT* enzymes other than *UGT1A1* or for other hepatic enzymes such as cytochrome P-450.

Experimental

NMR spectra were obtained at 500 MHz in $CDCl_3$ (unless otherwise noted), and chemical shifts are reported in ppm. UV-vis spectral data were determined in spectral grade solvents. Combustion analyses for carbon, hydrogen, nitrogen, and selenium were carried out by Desert Analytics, Tucson, AZ and gave results within $\pm 0.4\%$ of the theoretical values. Fast atom bombardment mass spectra were obtained from the Nebraska Center for Mass Spectrometry (Univ. Nebraska-Lincoln). GC-MS analyses were carried out on a capillary gas chromatograph (30 m DB-1 column) equipped with a mass selective detector. Analytical thin layer chromatography (TLC) was carried out on silica gel IB-F plates (125 µm layer); radial chromatography was carried out on silica gel PF_{254} with $CaSO_4$, preparative layer grade. For HPLC analyses, detection was in the range of ~410–460 nm, depending on the pigments being analyzed, and the column was an ultrasphere-IP 5 µm C-18 ODS column (25×0.46 cm) fitted with a similarly-packed precolumn (4.5×0.46 cm). The flow rate was 0.75–1.0 cm^3/min, the elution solvent

was 0.1 *M* di-*n*-octylammonium acetate in 2–8% aqueous methanol [14], and the column temperature ~34°C. Homozygous male *Gunn* rats, weighing 300–400 g, were obtained from our own colony and *Sprague-Dawley* male rats, weight 370–520 g, were obtained from local commercial vendors. Metabolism of **1** was investigated in three *Sprague-Dawley* rats and two homozygous *Gunn* rats. *In vivo* studies were done in a windowless room under safe lights following previously published procedures [11a, 23]. For these studies 0.25 mg of pigment were dissolved in 0.10 cm^3 of *DMSO* and this solution was mixed gradually with 1.0 cm^3 of rat serum. One cm^3 of the resulting solution was injected intravenously over 1 min *via* a femoral vein, and bile was collected in 20 mm^3 aliquots at frequent intervals from the tip of a short implanted biliary cannula over the next 240 min. Bile samples were flash frozen with dry ice and stored for less than a week at less than −50°C before being analyzed by HPLC. The synthesis and characterization of **4** are described elsewhere [14].

(4Z,15Z)-10-Selena-8,12-bis(2-carboxyethyl)-7,13-dimethyl-2,3,17,18-tetraethyl-(21H,23H,24H)-bilin-1,19-dione (**1**, $C_{34}H_{42}N_4O_6Se$)

To a 100 cm^3 3-neck round bottom flask, equipped with a nitrogen inlet, a magnetic stirrer, and a rubber septum were added 100 mg of 2-ethyl-neoxanthobilirubic acid (**5**) [8c] (0.33 mmol) and 30 cm^3 of CH_2Cl_2, and the system was flushed with N_2 for several min, while being chilled to 0°C using an ice-salt bath. To the stirred solution, 14.24 mm^3 of Se_2Cl_2 (38.9 mg, 0.17 mmol) in 1 cm^3 of CH_2Cl_2 were added dropwise using a syringe, and stirring was continued at 0°C. Product formation was noted at as early as 5 min into the reaction, but the reaction never went to completion, as determined from monitoring by TLC. Prolonged stirring or adding further portions of the Se_2Cl_2 reagent resulted in decomposition of the product. It was, therefore, decided to work up the reaction after half an hour, at which time ice-cold H_2O was added, and the resultant mixture was filtered to remove precipitated Se. The organic layer was washed with 3×30 cm^3 of H_2O, dried over anhyd. Na_2SO_4, filtered, and concentrated (rotovap). The dark residue was subjected to column chromatography on silica gel (increasing gradients of CH_2Cl_2:*Me*OH), and the least polar (yellow) and most polar (green) fractions were collected. Evaporation of solvent afforded 20 mg of the desired selena-rubin **1** and 60 mg of the starting dipyrrinone, which was dried and subjected to two more reaction cycles. Thus, 65 mg of the title rubin were obtained after three reaction cycles. Final purification was achieved by radial chromatography, which gave **1** as a brilliant yellow compound. Yield 60 mg (53%); mp > 250°C (dec); ^{1}H NMR (*DMSO*-d_6): $\delta = 1.03$ (t, $J = 7.5$ Hz, 6H), 1.10 (t, $J = 7.5$ Hz, 6H), 2.00 (s, 6H), 2.04 (q, $J = 7.5$ Hz), 2.24 (q, $J = 7.5$ Hz, 4H), 2.51 (t, $J = 8.5$ Hz, 4H), 2.66 (t, $J = 8.5$ Hz, 4H), 5.90 (s, 2H), 9.94 (brs, 2H), 10.76 (brs, 2H), 11.98 (brs, 2H) ppm; ^{1}H NMR ($CDCl_3$): $\delta = 1.09$ (t, $J = 7.5$ Hz, 7H), 1.15 (t, $J = 7.5$ Hz, 6H), 2.16 (s, 6H), 2.33 (s, 6H), 2.48 (q, $J = 7.5$ Hz, 4H), 2.6, 2.8, 2.9, 3.4 (4H, ABCX), 6.01 (s, 2H), 9.70 (brs, 2H), 10.84 (brs, 2H), 13.60 (brs, 2H) ppm; ^{13}C NMR in Table 1; UV: ε_{430}^{max} 45400 (acetone), ε_{439}^{max} 45900 (benzene), ε_{438}^{max} 45500 (chloroform), ε_{385}^{max} 37400, ε_{419}^{max} 39800 (*DMSO*), ε_{390}^{max} 38000, ε_{428}^{max} 46500 (methanol); FAB-MS (3-*NBA* matrix): 682 [$M^{+\bullet}$, $C_{34}H_{42}N_4OSe$].

Acknowledgment

We thank the National Institutes of Health (HD-17779, DK 26307, GM 36633, and P3O DK 26743) for support of this work. We also thank Ms. *W. Norona* for expert surgical and analytical assistance.

References

[1] McDonagh AF (1979) Bile Pigments: Bilatrienes and 5,15-Biladienes. In: Dolphin D (ed) The Porphyrins, vol 6. Academic Press, New York, pp 293–491
[2] Falk H (1989) The Chemistry of Linear Oligopyrroles and Bile Pigments. Springer, Wien
[3] a) Schmid R, McDonagh AF (1978) Hyperbilirubinemia. In: Stanbury JB, Wyngaarden JB, Fredrickson DS (eds) The Metabolic Basis of Inherited Disease, 4th ed. McGraw-Hill, New York,

pp 1221–1257; b) Berk PD, Noyer C (1994) Seminars Liver Dis **14**: 323; c) Chowdhury JR, Wolkoff AW, Chowdhury NR, Arias IM (2001) In: Scriver CR, Beaudet AL, Sly WS, Valle D (eds) The Metabolic and Molecular Bases of Inherited Disease, vol II. McGraw-Hill, New York, pp 3063–3101

[4] a) Bonnett R, Davies JE, Hursthouse MB, Sheldrick GM (1980) Proc R Soc London, Ser B, **B36**: 3007; b) Sheldrick WS (1983) Israel J Chem **23**: 155; c) Kaplan D, Navon G (1983) Israel J Chem **23**: 177

[5] Person RV, Peterson BR, Lightner DA (1994) J Am Chem Soc **116**: 42

[6] McDonagh AF, Lightner DA (1991) In: Bock KW, Gerok W, Matern S (eds) Hepatic Metabolism and Disposition of Endo and Xenobiotics (Falk Symposium No 57) chap 5 Kluwer, Dordrecht, The Netherlands, pp 47–59

[7] a) Paulusma C, Oude Elferink RPJ (1997) J Mol Med **75**: 420; b) Jedlitscky G, Leier I, Buchholtz U, Hummel-Eisenbeiss J, Burchell B, Keppler D (1997) Biochem J **327**: 305

[8] a) Xie M, Lightner DA (1993) Tetrahedron **49**: 2185; b) Thyrann T, Lightner DA (1995) Tetrahedron Lett **36**: 4345; c) Kar A, Lightner DA (1998) Tetrahedron **54**: 12671

[9] McDonagh AF, Lightner DA (1994) Cellular and Molecular Biology **40**: 965

[10] Chen Q, Huggins MT, Lightner DA, Norona W, McDonagh AF (1999) J Am Chem Soc **121**: 9253

[11] a) Tipton AK, Lightner DA, McDonagh AF (2001) J Org Chem **66**: 1832; b) Tipton A, Lightner DA (2002) Monatsh Chem **133**: 707

[12] a) Nogales D, Lightner DA (1995) J Biol Chem **270**: 73; b) Dörner T, Knipp B, Lightner DA (1997) Tetrahedron **53**: 2697

[13] The molecular dynamics calculations used to find the global energy minimum conformations of **1** were run on an SGI Octane workstation using v. 6.9 of the Sybyl forcefield as described in Ref. [5]. The Ball and Stick drawings were created from the atomic coordinates using *Müller* and *Falk*'s "Ball and Stick" program for the Macintosh (http://www.orc.uni-Linz.ac.at/mueller/ball_and_stick.shtml).

[14] Ghosh B, Lightner DA (2003) J Heterocyclic Chem **40**: 1113

[15] Iyanagi T, Watanabe T, Uchiyama Y (1999) J Biol Chem **264**: 21302

[16] Sato H, Aono S, Kashiwamata S, Koiwai O (1991) Biochem Biophys Res Commun **177**: 1161

[17] Clarke DJ, Keen JN, Burchell B (1992) FEBS Lett **299**: 183

[18] Ritter JK, Chen F, Sheen YY, Tran HM, Kimura S, Yeatman MT, Owens IS (1992) J Biol Chem **267**: 3257

[19] Coffman BL, Green MD, King CD, Tephly TR (1995) Mol Pharmacol **47**: 1101

[20] King CD, Green MD, Rios GR, Coffman BL, Owens IS, Bishop WP, Tephly TR (1996) Arch Biochem Biophys **332**: 92

[21] a) Zucker SD, Goessling W (2000) Biochim Biophys Acta-Biomembranes **1463**: 197; b) Wang P, Kim RB, Chowdhury JR, Wolkoff AW (2003) J Biol Chem **278**: 20695

[22] a) Kamisako T, Leier I, Cui YH, Konig J, Buccholz U, Hummel-Eisenbeiss J, Keppler D (1999) Hepatology **30**: 485; b) Kruh GD, Belinsky MG (2003) Oncogene **22**: 7537

[23] a) Brower JO, Lightner DA, McDonagh AF (2001) Tetrahedron **57**: 7813; b) McDonagh AF, Lightner DA, Nogales DF, Norona W (2001) FEBS Lett **506**: 211; c) McDonagh AF, Lightner DA, Kar AK, Norona WS (2002) Biochem Biophys Res Commun **293**: 1077; d) McDonagh AF, Lightner DA, Boiadjiev SE, Brower JO, Norona WS (2002) Bioorg Med Chem Lett **12**: 2483